

---

# Enhancing Laboratory-scale Flow Imaging of Fractured Geological Media with Deep Learning Super Resolution

---

Manju Pharkavi Murugesu<sup>1</sup> Timothy I Anderson<sup>2</sup> Niccoló Dal Santo<sup>3</sup> Vignesh Krishnan<sup>4</sup>  
Anthony R Kovscek<sup>1</sup>

## Abstract

Injection into deep geological formations is a promising approach for the utilization, sequestration, and removal from the atmosphere of CO<sub>2</sub> emissions. Laboratory experiments are essential to characterize how CO<sub>2</sub> flows and reacts in various types of geological media. We reproduce such dynamic injection processes while imaging using Computed Tomography (CT) at sufficient temporal resolution to visualize changes in the flow field. The resolution of CT, however, is on the order of 100's of  $\mu\text{m}$  and insufficient to characterize fine-scale reaction-induced alterations to micro-fractures. Super resolution deep learning is, therefore, an essential tool to improve spatial resolution of dynamic CT images. We acquired and processed pairs of multi-scale low- and high-resolution CT rock images. We also show the performance of our baseline model on fractured rock images using peak signal to noise ratio and structural similarity index. Coupling dynamic CT imaging with deep learning results in visualization with enhanced spatial resolution of about a factor of 4 thereby enabling improved interpretation.

## 1. Introduction

Low-carbon energy resources and large-scale greenhouse emissions reductions are important to meet the global demand for energy while combating climate change. Subsurface geology provides large scale solutions to our climate goals through technologies such as CO<sub>2</sub> utilization and sequestration, subsurface hydrogen and compressed air stor-

<sup>1</sup>Department of Energy Resources Engineering, Stanford University, California, USA <sup>2</sup>Department of Electrical Engineering, Stanford University, California, USA <sup>3</sup>The MathWorks Ltd, Cambridge, UK <sup>4</sup>The MathWorks Ltd, Natick, Massachusetts, USA. Correspondence to: Anthony R Kovscek <kovscek@stanford.edu>.

age, and enhanced geothermal systems. For example, CO<sub>2</sub> can replace water in hydraulic fracturing processes while simultaneously sequestering, creating a reduced-carbon or carbon negative energy process (Middleton et al., 2015; Pruess, 2006).

Injected CO<sub>2</sub> tends to flow preferentially through naturally existing or induced fractures. CO<sub>2</sub> and brine mixtures are quite acidic. The low pH brine chemically interacts with surface minerals along fractures, altering rock-fluid interactions through dissolution and precipitation of certain rock minerals. Such reactions can significantly impact the porosity and permeability along the fractures and near-fracture matrix, affecting both CO<sub>2</sub> flow and storage processes. Visualization techniques, such as Computed Tomography (CT) imaging, capture alterations of fractures during reactive transport experiments at the laboratory scale.

CT is an important technique to image rocks during dynamic transport experiments. The resolution of CT images, however, is insufficient to characterize accurately the changes in fractures and rock matrix porosity on the order of  $\mu\text{m}$  or less. Micro-CT ( $\mu\text{CT}$ ) scanners have the necessary superior resolution to characterize reactive transport processes at the microscale. The scan time of  $\mu\text{CT}$  is longer than that of a CT by at least an order of magnitude and therefore limits the temporal resolution significantly.

To overcome these challenges, we propose to image dynamic reactive transport using CT scanners and later upsample the CT image to have comparable resolution to  $\mu\text{CT}$ . Dong et al. (2015) shows that deep convolutional neural networks (CNN) are state of the art superior methods for image super resolution tasks. Past literature reports supervised super resolution deep learning models based on micro-CT and synthetically downsampled micro-CT image pairs for geological samples (Wang et al., 2019; Da Wang et al., 2019; Chen et al., 2020). Low-resolution CT images are more applicable inputs to super resolution deep learning models due to the widespread use of CT in geoscience. The availability of CT and micro-CT imaging capability motivates us to train CNN models with low resolution CT as input images and high-resolution micro-CT as ground truth images. Hence, this work extends super resolution deep learning for

multi-scale data obtained from separate imaging platforms.

## 2. Proposed Workflow

We propose the workflow shown in Figure 1 to conduct neural network super resolution of multi-scale CT rock images. The workflow outlines the steps to prepare images, train models and later effectively deploy the models for our application.

**Image acquisition:** We imaged cylindrical rock samples in both CT and micro-CT under ambient conditions. The resolutions of rock images obtained from CT and micro-CT are  $195\mu\text{m} \times 195\mu\text{m} \times 625\mu\text{m}$ , and  $27\mu\text{m} \times 27\mu\text{m} \times 27\mu\text{m}$  respectively. Despite the resolution difference, we prefer to use CT images for our dynamic transport experiments due to the shorter scan time of CT in the range of minutes. The 3D rock images in Figure 1 show two fractures extending from either side of the core. The CT image overestimates the actual fracture aperture.

**Image pre-processing:** Image pre-processing is crucial for curating a dataset for deep learning single image super resolution. We align the images using the pipeline outlined in Figure 2. The distribution of pixels in the CT and micro-CT images are approximately similar at the end of the pre-processing step.

**Model training:** We use feed-forward deep SR-ResNet generator adapted from [Ledig et al. \(2017\)](#). Due to homogeneity of rock images, it is important that the model is sensitive to fine details and produces realistic looking matrix structure. Super resolution generative adversarial network (SR-GAN) addresses this problem by incorporating an additional discriminator network that pushes the synthesized images towards the manifold of natural images ([Ledig et al., 2017](#)). Although the images for this study are all obtained from CT-based instruments, image contrast is possibly offset due to default settings of the separate CT and  $\mu$ CT machines. Therefore, the project adapts the multimodal image enhancement implementation suggested by [Anderson et al. \(2020\)](#) based on the Pix2pix conditional GAN model ([Isola et al., 2017](#); [Zhu et al., 2017](#)). For initial 2D super resolution, we randomly sampled  $64 \times 64$  patches in CT images and their  $256 \times 256$  micro-CT pairs. Preliminary training based on hyperparameters recommended by [Isola et al. \(2017\)](#) is conducted with different loss functions such as L1 loss, Wasserstein GAN loss and vanilla GAN loss. The common hyperparameters between the different models are shown in Table 1.

Initial results for a validation set are shown in Figure 3. For the purpose of initial study, the images are evaluated offline after the acquisition. Peak signal to noise ratio (PSNR) measures the proportion between maximum signal power and the mean squared error, and structural similarity index

Table 1. Model Parameters

Model Parameter	Choice
Training data size	10,000
Validation data size	100
Test data size	100
Initial learning rate	0.0002
Optimization	Adam
Normalization	Instance
Batch size	1
Number of epochs	20

measure (SSIM) quantifies the structural difference between two images.

The feedforward SR-CNN model shows the greatest PSNR and SSIM. However, the matrix structure of the rocks are washed out because the L1 loss function tends to better distinguish the main features and renders other details sparsely. The conditional GAN predictions look more realistic because the discriminator drives the model to predict perceptually realistic looking images. Therefore, We propose to formulate an ensemble model combining the SR-CNN and conditional GAN for future analysis. Note the artifact in the GAN-predicted image. Checkerboard artifacts are also reported for GAN-predicted fake images during upsampling in previous studies ([Zhang et al., 2019](#); [Zhu et al., 2019](#)).

## 3. Ongoing Work

Once the model is trained, we propose to deploy directly the model during each time step of the dynamic reactive transport process. The combination of rapid CT imaging and super resolution deep learning models allows us to visualize dynamic transport experiments with high spatial and temporal resolution. The enhanced visualization accurately characterizes fractures and porosity of the geological formation rocks that are in consideration for  $\text{CO}_2$  and  $\text{H}_2$  storage processes as well as enhanced geothermal systems. We plan to analyze in detail the uncertainty of the pixel resolution outcome of the model with images obtained during dynamic transport experiments.

## 4. Path to Climate Impact

Figure 4 shows the path of this proposal to meaningful climate impact. The 3D image shows the CT-segmented fractures of a geologic rock at laboratory scale. Enhanced visualization of transport processes in fractured rock with greater spatial and temporal resolutions allows for more accurate segmentation of the fractures and porosity of the core. Such information is foundational to modeling of transport and reaction. Additionally, accurate characterization of the

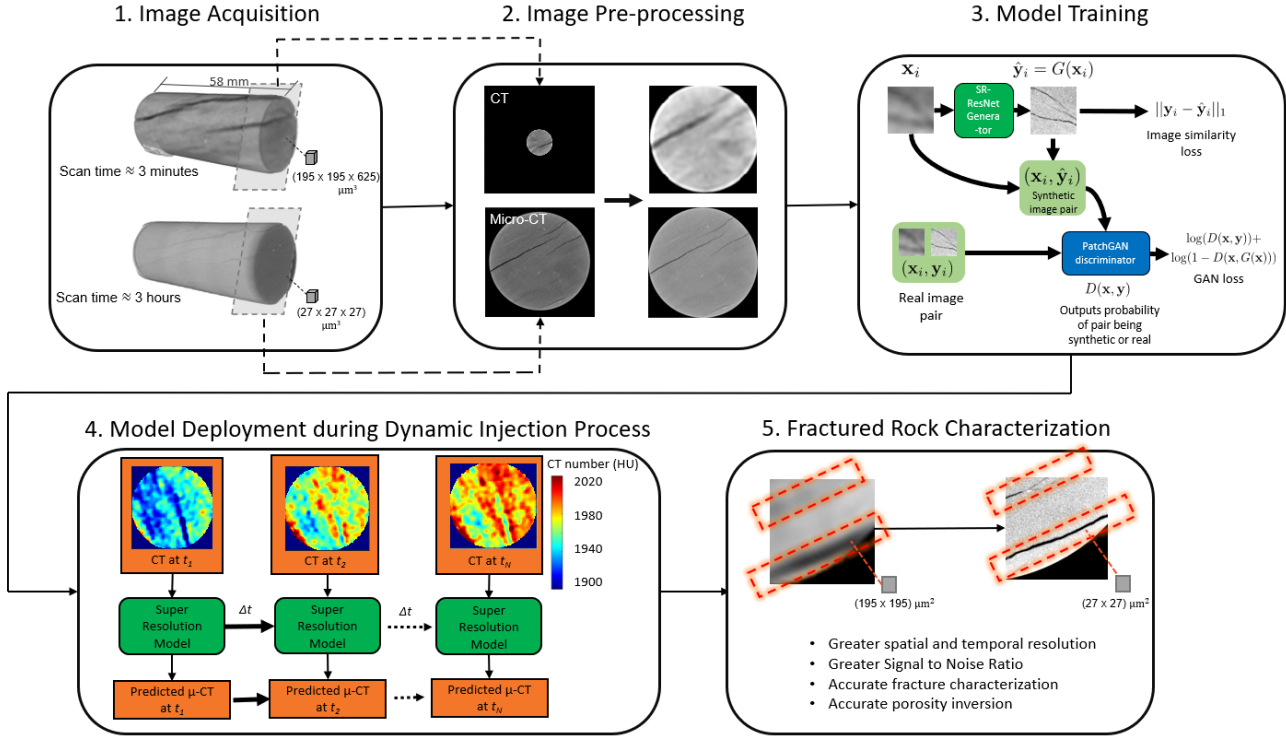


Figure 1. Proposed workflow for application of machine learning to characterize better fractured geologic porous media using enhanced visualization during dynamic injection processes.

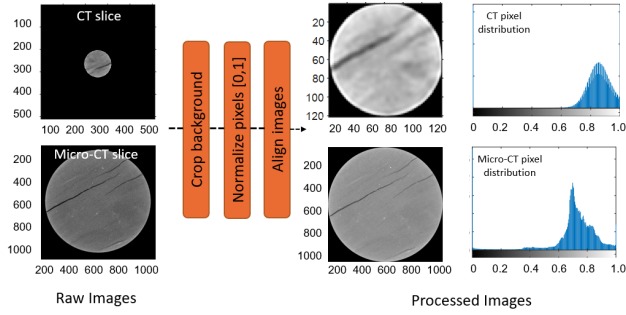


Figure 2. Image pre-processing pipeline for CT and micro-CT images of the same volume.

formation rock guides selection of geological formations for CO<sub>2</sub> injection and appropriate technology for monitoring of fluid storage. This study significantly reduces the uncertainties encountered during subsurface injection and monitoring and will enable new insights into carbon emission reduction strategies and safe implementation of these technologies.

## References

Anderson, T. I., Vega, B., and Kovscek, A. R. Multimodal imaging and machine learning to enhance microscope

images of shale. *Computers & Geosciences*, 145:104593, 2020.

Chen, H., He, X., Teng, Q., Sheriff, R. E., Feng, J., and Xiong, S. Super-resolution of real-world rock microcomputed tomography images using cycle-consistent generative adversarial networks. *Physical Review E*, 101(2): 023305, 2020.

Da Wang, Y., Armstrong, R. T., and Mostaghimi, P. Enhancing resolution of digital rock images with super resolution convolutional neural networks. *Journal of Petroleum Science and Engineering*, 182:106261, 2019.

Dong, C., Loy, C. C., He, K., and Tang, X. Image super-resolution using deep convolutional networks. *IEEE transactions on pattern analysis and machine intelligence*, 38(2):295–307, 2015.

Isola, P., Zhu, J.-Y., Zhou, T., and Efros, A. A. Image-to-image translation with conditional adversarial networks. In *Proceedings of the IEEE conference on computer vision and pattern recognition*, pp. 1125–1134, 2017.

Ledig, C., Theis, L., Huszár, F., Caballero, J., Cunningham, A., Acosta, A., Aitken, A., Tejani, A., Totz, J., Wang, Z., et al. Photo-realistic single image super-resolution using a generative adversarial network. In *Proceedings*

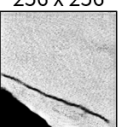
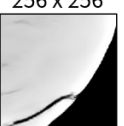
Model	Low resolution	Ground truth	Predicted image	Quantitative Metrics
Conditional GAN Wasserstein loss	 64 x 64	 256 x 256	 256 x 256	PSNR: $15.957 \pm 0.190$ SSIM: $0.148 \pm 0.010$
Conditional GAN vanilla loss	 64 x 64	 256 x 256	 256 x 256	PSNR: $18.657 \pm 0.369$ SSIM: $0.210 \pm 0.007$
Feedforward CNN L1 loss	 64 x 64	 256 x 256	 256 x 256	PSNR: $19.587 \pm 0.266$ SSIM: $0.228 \pm 0.009$

Figure 3. Preliminary results for 2D super resolution based on different loss functions.

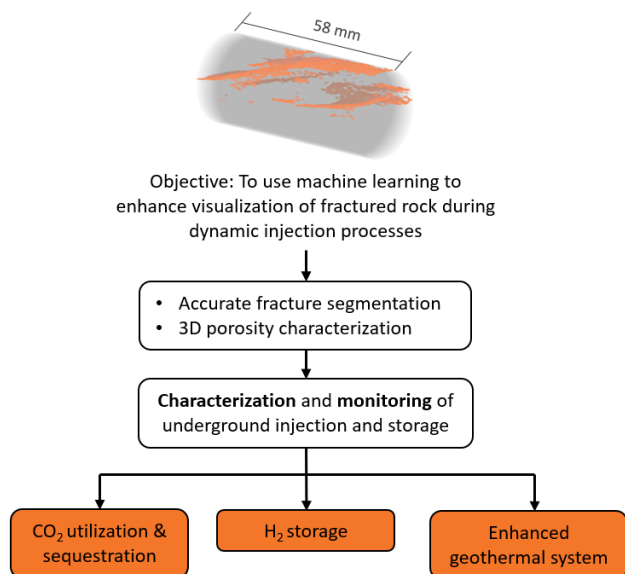


Figure 4. Path to climate impact: Enhanced visualization of dynamic injection processes of fractured rock allows for better characterization and monitoring of CO<sub>2</sub> and H<sub>2</sub> injection and sequestration.

of the IEEE conference on computer vision and pattern recognition, pp. 4681–4690, 2017.

Middleton, R. S., Carey, J. W., Currier, R. P., Hyman, J. D., Kang, Q., Karra, S., Jiménez-Martínez, J., Porter, M. L., and Viswanathan, H. S. Shale gas and non-aqueous fracturing fluids: Opportunities and challenges for supercritical co<sub>2</sub>. *Applied Energy*, 147:500–509, 2015.

Pruess, K. Enhanced geothermal systems (egs) using co<sub>2</sub> as working fluid—a novel approach for generating renewable energy with simultaneous sequestration of carbon. *Geothermics*, 35(4):351–367, 2006.

Wang, Y., Teng, Q., He, X., Feng, J., and Zhang, T. Ct-image of rock samples super resolution using 3d convolutional neural network. *Computers & Geosciences*, 133:104314, 2019.

Zhang, X., Karaman, S., and Chang, S.-F. Detecting and simulating artifacts in gan fake images. In *2019 IEEE International Workshop on Information Forensics and Security (WIFS)*, pp. 1–6. IEEE, 2019.

Zhu, J., Yang, G., and Lio, P. How can we make gan perform better in single medical image super-resolution? a lesion focused multi-scale approach. In *2019 IEEE 16th International Symposium on Biomedical Imaging (ISBI 2019)*, pp. 1669–1673. IEEE, 2019.

Zhu, J.-Y., Park, T., Isola, P., and Efros, A. A. Unpaired image-to-image translation using cycle-consistent adversarial networks. In *Proceedings of the IEEE international conference on computer vision*, pp. 2223–2232, 2017.